# OPTICAL FBG SENSORS FOR STATIC STRUCTURAL HEALTH MONITORING

Paulo Antunes [1,2*], Humberto Varum [3], Paulo André [1,2†]

[1] *Instituto de Telecomunicações, Portugal*
[2] *Departamento de Física da Universidade de Aveiro, Portugal*
[3] *Departamento de Engenharia Civil da Universidade de Aveiro, Portugal*

## ABSTRACT

In this paper, the monitoring of an adobe structure with optical fiber sensors is reported. Static measurements were made during a destructive test on a full-scale wall, in which an in-plane cyclic force was imposed by a hydraulic jack until its collapse. The recorded data with these sensors and the force applied evolution allows to identify the two instants when the major diagonal cracks occur in the wall. Initially, before the cracking, a linear elastic response was observed, corresponding to a deformation at each monitoring point proportional to the applied lateral force, being quantified the relation between the external force and the deformation at each point. This structural test allows demonstrating the feasibility of applying static optical FBG sensors to study the behavior and performance of civil engineering infrastructures even for extreme loading events.

**Keywords:** Optical fibers, FBGs, Sensors, Adobe masonry walls, Destructive full-scale test.

## 1. INTRODUCTION

Nowadays structural health monitoring is a fundamental tool to assess the behavior of existing structures but also to control the performance of large new structures, foreseen to give information to monitor their lifetime. In this paper, the monitoring of a full-scale adobe masonry structure (I-shaped in plan) with optical fiber sensors is reported. Static measurements were made during a destructive test on the adobe wall, in which an in-plane horizontal cyclic force was imposed by a hydraulic actuator until its collapse. A network of thirteen multiplexed displacement sensors was used. The used optical sensors are based in Fiber Bragg Gratings (FBG) recorded in standard single mode optical fibers. Since FBG sensors are an all-in-fiber technology, they take advantage of the optical fiber properties, presenting also advantages over traditional electronic sensors due to the possibility to multiplex a large number of different sensors (temperature, displacement, pressure, pH value, humidity, high magnetic field and acceleration) into the same optical fiber, reducing the need for multiple and heavy cabling used in traditional electronic sensing (Antunes et al., 2009).

* Corresponding author: Email: pantunes@ua.pt

† Presenter: Email: pandre@av.it.pt

Other advantage of the optical sensors is the inherent fact that the information is codified in the optical domain, so, this kind of sensors can be used in hostile environments, where electrical currents of electronic devices might pose a hazard. Many applications has been found for this type of sensors in structural sensing: strain monitorization in civil infrastructures; pile load monitoring; strain monitoring in reinforced concrete beams; early age cement shrinkage; strain monitoring in smart structures; moisture and humidity measurements in civil applications; geodynamic applications; ultrasonic non-destructive testing of structural health are among their numerous applications, see (Majumder et al., 2008) and references therein.

## 2. FIBER BRAGG GRATINGS

A FBG is a passive optical device which is based in the modulation of the optical fiber core refractive index. The modulation on the refractive index can be produced exposing a photosensitive optical fiber to an intense pattern of ultraviolet light, which can be created by a phase mask or by a interferometric process. The refractive index modulation is equivalent to a set of reflection planes perpendicular to the longitudinal axis of the fiber (Othonos and Kalli, 1999). When the FBG is illuminated by a spectral broad optical source, a spectral slice of the incident radiation is successively reflected on the reflection planes, being the remaining signal transmitted. The reflected spectrum is a narrow spectral band, centred at the Bragg wavelength, $\lambda_B$, given by the first order Bragg condition (Othonos and Kalli, 1999):

$$\lambda_B = 2 n_{ef} \Lambda \tag{1}$$

where $n_{ef}$ is the effective refractive index of the optical fiber and $\Lambda$ the periodicity of the created modulation. The Bragg condition declares a temperature and strain dependence of $\lambda_B$, implicit due to the dependence of $n_{ef}$ and $\Lambda$ on the temperature and mechanical deformation. If the fiber is compressed/stretched or exposed to temperature variations it will induce a shift on the reflection spectrum, which is proportional to the neighbouring variation. The dependency of the Bragg wavelength on temperature and strain can be described by (Antunes et al., 2009):

$$\Delta\lambda_B = 2\left(\Lambda \frac{\partial n_{eff}}{\partial l} + n_{eff} \frac{\partial \Lambda}{\partial l}\right)\Delta l + 2\left(\Lambda \frac{\partial n_{eff}}{\partial T} + n_{eff} \frac{\partial \Lambda}{\partial T}\right)\Delta T \tag{2}$$

The first term in equation (2) represents the strain effect on $\lambda_B$ and can be expressed by equation (3). The second term in equation (3) represents the dependence on $\lambda_B$ due to temperature and can be expressed by equation (4):

$$\Delta\lambda_B = \lambda_B \left[1 - \frac{n_{eff}^2}{2}[p_{12} - \upsilon(p_{11} + p_{12})]\right]\varepsilon_z \tag{3}$$

$$\Delta\lambda_B = \lambda_B \left[\alpha_\Lambda + \alpha_n\right]\Delta T \tag{4}$$

where $\nu$ stands for the silica Poisson ratio, $p_{11}$ and $p_{12}$ are components of the strain-optic tensor, $\alpha_\Lambda$ is the thermal expansion coefficient and $\alpha_n$ the thermo-optic coefficient. For Germanosilicate core doped optical fibers and for a wavelength of 1550 nm, the typical values for the strain and thermal sensitivities are 1.2 pm/με and 13 pm/ºC, respectively (Othonos and Kalli, 1999).

## 3. EXPERIMENTAL SETUP

To demonstrate the application of FBG on the static measurements for structural health monitoring (SHM), a full-scale wall mockup was build with adobe blocks. The adobe blocks were obtained from a dwelling demolition on Aveiro region, Portugal. The blocks have average dimensions of 29×45×12 $cm^3$, with volumetric weight of 16 $kN/m^3$. The wall model is I-shaped, with a height of 3.07 m, length of 3.50 m and thickness of 0.29 m, being representative of typical adobe constructions in the region, and is plastered on both sides of each wall element. To fix the wall to the base, concrete blocks connected by steel pre-stressed rods to the reaction-floor of the laboratory were used. The first layer of adobe blocks was settle with cement mortar, preventing joint slippage at this point during the test. An additional vertical load of 2 tons was placed over the wall, to simulate other dead-loads (pavements, roofs) and live-loads (Pereira, 2008). The test was conducted with the imposition of cyclic in-plane horizontal forces of increasing amplitude taxes on the top of the wall until its collapse.

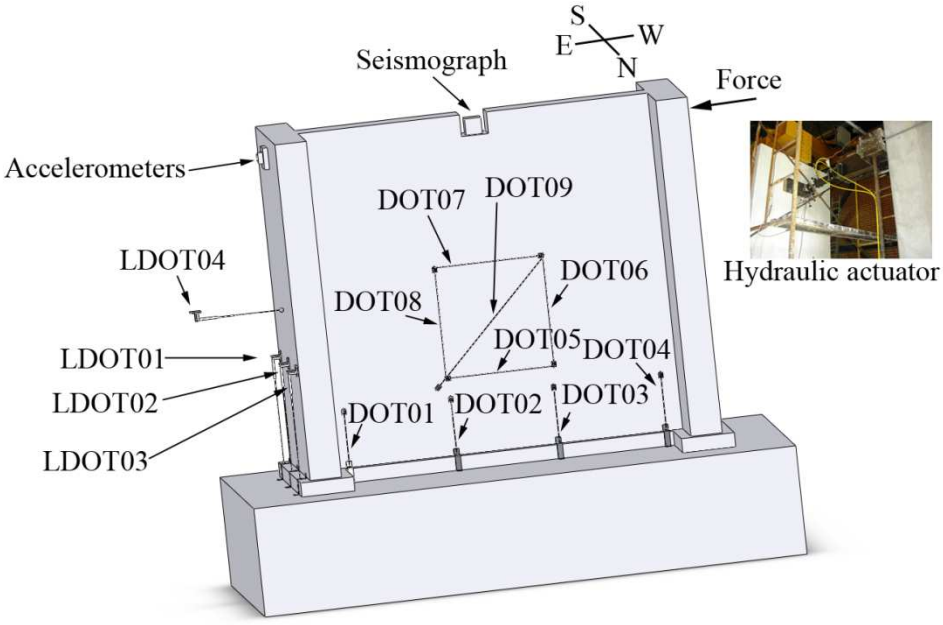


**Figure 1: Scheme of the wall and location of the optical sensors and hydraulic actuator.**

In order to measure the relative deformation at various points in the wall caused by the application of horizontal cyclic loading, thirteen displacement sensors were installed based on fiber Bragg gratings. Of these, nine were developed in the Department of Physics, University of Aveiro (DOT01, ..., DOT09) and the remaining four are commercial solutions (LDOT01, ..., LDOT04). The optical sensors were placed in the adobe structure in accordance with the distribution schematized in Figure 1 (left), measuring the relative displacement between two points (deformation in the horizontal, vertical or diagonal direction).

On the North face were installed the nine optical sensors developed in our laboratory, identified by: DOT01, DOT02, DOT03 and DOT04 for sensors sensitive to vertical deformation at the base of the wall, and DOT05, DOT06, DOT07, DOT08 and DOT09 for sensors used in monitoring of a central portion of the wall. On the East face of the structure four commercial optical sensors were used, sensors LDOT01, LDOT02 and LDOT03 were used for monitoring vertical movements of the base of the wall and sensor LDOT04 in monitoring horizontal movements of the wall in the West-East direction at a height of 1.47 m. Each developed sensor consist of an optical fiber with a Bragg grating inscribed, fixed on two supports, one fix and the other movable. The latter allows to apply a pre-determined tension, thus enabling measure not only relative expansion but also contraction of the points monitored on the structure. The fix point is attached to the rigid foundation of the structure and not to the wall-base itself. In this way relative deformations are measured from the point of the movable sensor support to the rigid base of the wall.

The sensor network was multiplexed through three optical fibers. A first optical fiber connecting the sensors LDOT01, LDOT02, LDOT03 and LDOT04 dedicated to the measurement of global displacements of points in the East face of the wall, a second optical fiber collects the signal from the sensors of the central core of the wall at the North face (DOT05, DOT06, DOT07, DOT08 and DOT09) and a third optical fiber collects the signal from the sensors at the base of the North face (DOT01, DOT02, DOT03 and DOT04). The three optical fibers are multiplexed using a 1 × 3 coupler and the signal is measured at a rate of 1 sample per second. The FBGs produced and used in this paper were printed in monomode photosensitive fiber (FiberCore PS1250/1500) with a KrF excimer laser at 248 nm using the technique of phase mask. They have a length of 3 mm and a mean optical rejection of 25 dB. Each FBG was written with a different Bragg wavelength, namely: 1531 nm, 1535 nm, 1538 nm, 1543 nm, 1546 nm, 1552 nm, 1559 nm, 1561 nm and 1564 nm. Before use, the FBGs were characterized to deformation and temperature variations. To characterize to the temperature variations, the fiber with the Bragg grating was placed on a thermoelectric module and covered with a heat sink compound to smooth the progress of heat transfer. The thermoelectric module was commanded by a controller model ThorLabs TED 350, using an LM335 temperature sensor. To characterize to the deformation variations, the fiber with the FBG was attached to a fixed support at one end and to a linear transducer device at the other end, which allow applying a controllable tension. In both types of characterization, the Bragg wavelength was

monitored by an interrogation unit SM125 from Micron Optics. It was obtained a value of 1.18±0.02 pm / με for the sensitivity to strain. This value will then be used to convert the measured shift of the Bragg wavelength associated to the relative displacement of the points on the wall at each monitoring position. The temperature sensitivity was measured by the linear fit of the wavelength data as a function of temperature, leading to a value of 8.72±0.06 pm/ºC. However, the tests described in the wall had duration of less than 1 hour, occurring within a time interval that does not produce a significant variation of temperature, thus it was neglected the effect of temperature variation on the sensors.

The horizontal cyclic force was imposed in the direction West-East by a hydraulic actuator fixed on the West face of the wall specimen. The hydraulic actuator was placed at a height of 2.5m above the base of the wall and is fixed to a reaction-wall lying W of the tested adobe wall. The cyclic force imposed by the actuator was measured with a load-cell type TC4, brand AEP Transducers, simultaneously with the recording of relative displacements at various points through electronic transducers. The evolution of the applied force over time during the test is shown in Figure 2 (left).

## 4. RESULTS

The sensor LDOT04 measures the horizontal displacement in the direction of loading. The evolution of the displacements recorded by this sensor and of the force applied are presented in Figure 2 (left), as well as the identification of the two instants in which the two main cracks are produced on the wall. The first occurs at 1847 s of the test duration and the second at 2032 s.

In Figure 2 (right), the maximum (positive and negative) displacements recorded in the vertical sensors at the E face of the wall are represented, noting that the largest displacements occur in the sensor located in the center. Given the I-shape of the wall and load applied concentrated in the web plane, this result is rational since larger stresses are installed in the web alignment.

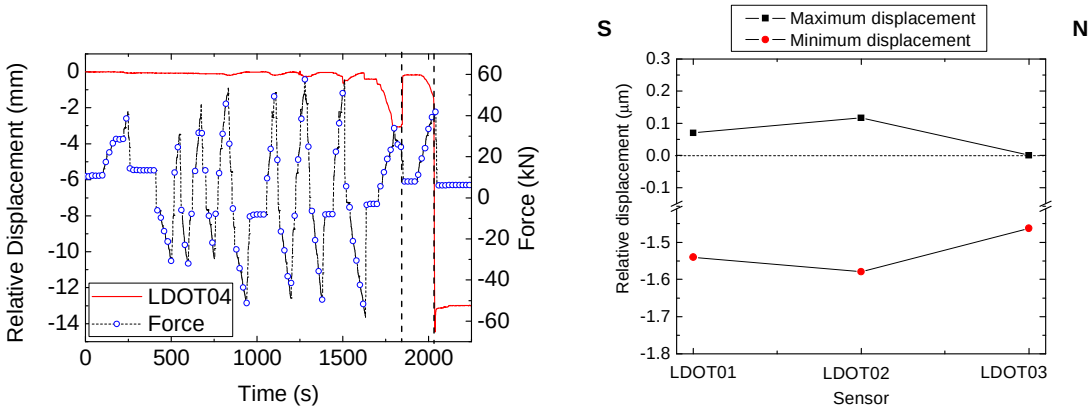


**Figure 2: Evolution of the displacement recorded at sensor LDOT04 and evolution of the horizontal force imposed (left) and maximum (positive and negative) displacement measured on the face E sensors (right).**

The measurements obtained with the optical sensors located at the North face of the wall base are illustrated in Figure 3 (left), where the evolutions of the horizontal relative displacement of two points at the centre of the wall web, measured with the optical sensor DOT05, and of the cyclic force applied are represented. At the instant 1650 s of the test, an offset is recorded in the displacement sensor, which is in agreement with the diagonal crack observed in the measurement area of the sensor.

In Figure 3 (right) is represented the maximum (positive and negative) vertical displacement recorded with sensors at the base of the wall in the face N, throughout the test. It is observed that the point where the largest displacement occurs is the one closest to the side of the wall where the concentrated horizontal load is applied, due to the aperture of an horizontal fissure at this point of the base for a force towards W to E. The maximum deformation recorded in the opposite point (DOT01) corresponds to compression deformations.

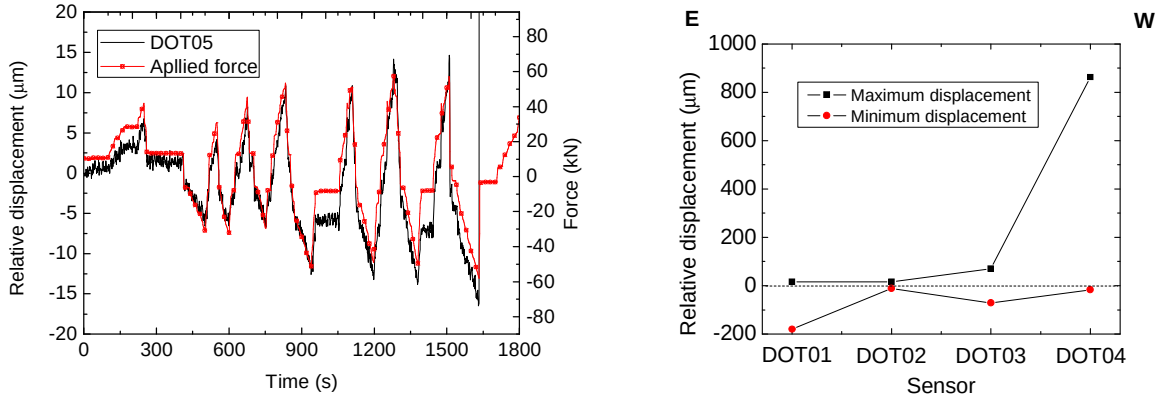


**Figure 3: Relative displacement evolution at sensor DOT05 and horizontal cyclic force histories (left) and maximum (positive and negative) displacement measured at the base of the wall - face N (right).**

Initially, before cracking, a linear response regime is observed, corresponding to an elastic deformation distribution, proportional to the lateral force applied. In this initial elastic regime is possible to quantify the relationship between external force and the horizontal deformation at each point monitored by a linear fit of the data. When the external force is applied from West to East, positive vertical deformations corresponding to elongation are recorded at the West side of wall and contraction at the opposite side. The ratio between the applied force and the vertical displacement measured at each point in the base of the wall is proportional to the distance of the corresponding point to the centre of the wall base. This is shown in Figure 4, where a linear relation with a slope of $0.168 \pm 0.033$ µ m kN $^{-1}$ m$^{-1}$ was obtained. Indeed, this behaviour represents the bending deformation component of the wall at its base.

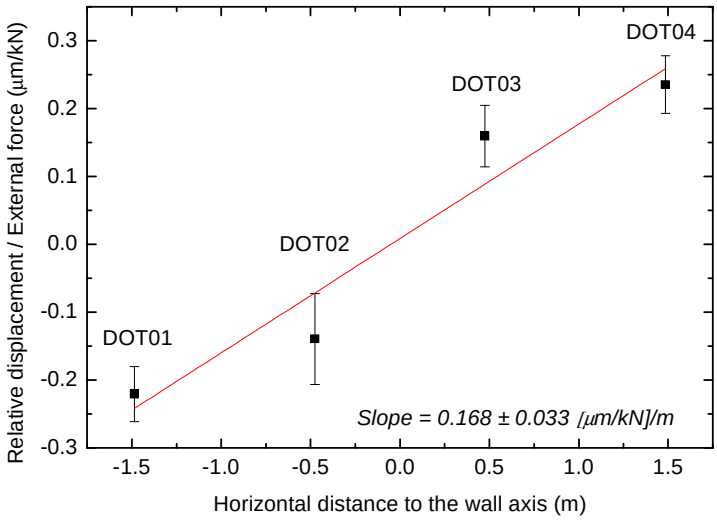


**Figure 4: Ratio between the relative displacement at the wall base and the external force against the horizontal distance of the monitoring points to the central axis of the wall. Dots represent the experimental data and the line the linear fit (correlation factor of 0.920).**

The group of sensors placed in the central part of the North face of wall allowed the identification and monitoring of the most important damage observed in the adobe structure during the cyclic test. Figure 5 shows a detail of the sensors location and the main diagonal cracks observed at the end of the test. In Figure 5 are also identified the support points of the sensors, designated 1 to 4.

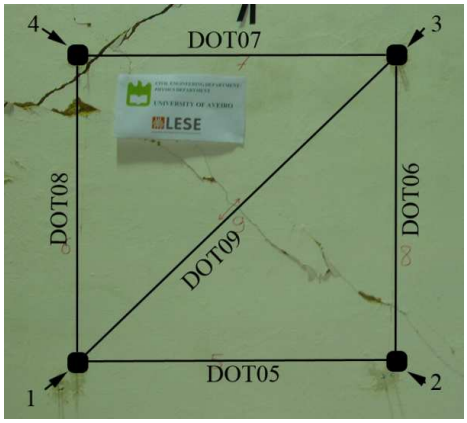


**Figure 5: Location of the sensors at the center of the N face of the wall and main cracks observed.**

From the data recorded with a group of sensors, it was possible to identify and estimate the relative motion of the monitored points. For this analysis, the point 1 was considered as a fix reference point and the vertical displacement of point 2 was neglected. The relative movement along the vertical

and horizontal axis of points 3 and 4, depending on the external force applied are represented in Figure 6 (left) and (right), respectively. The largest movement occurs, as expected, in the horizontal direction. However, throughout the test and with the progress of damage in the wall, are also observed relevant vertical movements in points 3 and 4. For point 3, after the diagonal cracking of the wall, a peak displacement in the horizontal direction is also observed. The information and conclusions are consistent with the pattern of damage and cracking observed on the wall during the test.

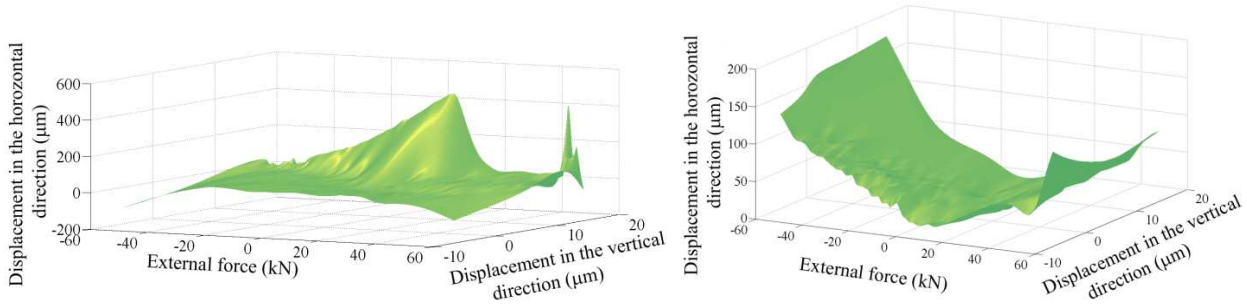


**Figure 6: Evolution of the relative displacement during the cyclic test for point 3 (left) and for point 4 (right) (the data was interpolated within the experimental data to be represented as a surface).**

## 5. CONCLUSIONS

The study showed the applicability of optical sensors for monitoring static and dynamic structures. A network of thirteen displacement sensors has been implemented successfully and interrogated, allowing to monitor a destructive test performed on a full-scale adobe wall.

## ACKNOWLEDGMENTS

Paulo Antunes and Humberto Varum acknowledge the financial support from Fundação para a Ciência e Tecnologia (FCT) through the Ph.D fellowship SFRH/BD/41077/2007 and the sabbatical leave fellowship SFRH/BSAB/939/2009, respectively.

## REFERENCES

Antunes PFC, Lima HFT, Alberto NJ, et al. (2009) Optical Fiber Accelerometer System for Structural Dynamic Monitoring. *Sensors Journal, IEEE,* **9,** 1347-1354.

Majumder M, Gangopadhyay TK, Chakraborty AK, Dasgupta K, Bhattacharya DK (2008) Fibre Bragg gratings in structural health monitoring--Present status and applications. *Sensors and Actuators A: Physical,* **147,** 150-164.

Othonos A, Kalli K (1999) *Fiber Bragg Gratings: Fundamentals and Applications in Telecommunications and Sensing,* Artech House.

Pereira H (2008) Caracterização do comportamento estrutural de construções em adobe. *MSs thesis in civil engineering, Universidade de Aveiro, Aveiro.*